LA-UR-19-22131
Approved for public release; distribution is unlimited.

Title: SESAME 2985: A new molybdenum equation of state table

Author(s): Bjorgaard, Josiah August
Wills, John Michael
Crockett, Scott
Sheppard, Daniel Glen

Intended for: Report

Issued: 2019-03-11

SESAME 2985: A new molybdenum equation of state table

J. A. Bjorgaard,[1, a)] J. Wills,[2, b)] S. Crockett,[2, c)] and D. Sheppard[1, d)]
[1)] *XCP-5, Los Alamos National Laboratory, Los Alamos, NM*
[2)] *T-1, Los Alamos National Laboratory, Los Alamos, NM*

(Dated: 30 January 2019)

PACS numbers: Valid PACS appear here
Keywords: equation of state, molybdenum

Molybdenum is a body centered-cubic metal with a variety of high technology applications due to it's thermal, mechanical, and chemical stability. In high pressure research, it is used as a calibration standard in diamond anvil cell (DAC) measurements. Many theoretical and experimental studies have been performed to study the Mo equation of state (EOS) to high pressure.[1–3]

The LANL SESAME database includes tabulated equations of state for many materials from ambient conditions to high pressure and temperature.[4] The last update to the Mo SESAME table was in 1998 and was numbered 2984. Since then, new shock, compression, and melt line data has become available.[5–7] Furthermore, density functional theory (DFT) models have been improved and their application to high pressure and temperature EOS simulations has evolved in recent years.[8–11] In this report, we detail a new Mo SESAME table numbered 2985. It includes new cold curve DFT calculations a better tuned melt line. This allows us to better match shock Hugoniot data.

SESAME 2984 was prepared with the GRIZZLY code, the predecessor to openSESAME. OpenSESAME includes better interpolation schemes and the ability to include a Maxwell construction table to correct for the inherent van der Waals loop.[12] The cold curve in SESAME 2984 was determined directly from matching a selection of shock data, but does not agree with experiments in the ultra-high pressure regime.[5] For these reasons, we have developed SESAME 2985, which comprises our best description of the Mo EOS using all available experimental data.

The SESAME equation of state is defined by three additive contributions

$$U(\rho, P, T) = U_{T=0}(\rho, P) + U_{ion}(\rho, P, T) + U_{elec}(\rho, P, T) \quad (1)$$

where $U_{T=0}$ is the cold curve, U_{ion} is the ionic component, and U_{elec} is the electronic component. U_{elec} uses the Thomas-Fermi-Dirac method to describe electronic excitation.[4]

For $U_{T=0}$ we have chosen a Burch-Murnaghan EOS (taking terms up to 7th order). This is fit to DAC measurements and DFT calculation (Fig. 1). For DFT, the linearized-muffin tin orbital method[13] with the AM05 functional[14] was used to determine the cold curves of bcc, fcc, and hcp Mo to ultra-high pressure. The different phases had a small energy difference at high pressure, on the same scale as the error in the Burch-Murnaghan EOS fit. For simplicity, we have decided to include only the bcc phase in the EOS table. Other full-potential calculations of Mo predict a phase transformation to fcc at around 660 GPa,[9] but we expect this to have little effect on the final SESAME table. Surveying the available literature, mixed phases may occur at high pressure.[7] The DFT cold curve is shifted to lower pressure by 15 GPa in order to match the experimental DAC data. The DAC data, measured at room temperature by Dewaele et al.[15], is extrapolated to 0K in Ref. 6. The 0K density of 10.335 g/cm^3 and bulk modulus of 266 GPa are used as the basis for the Burch-Murnaghan EOS fit.

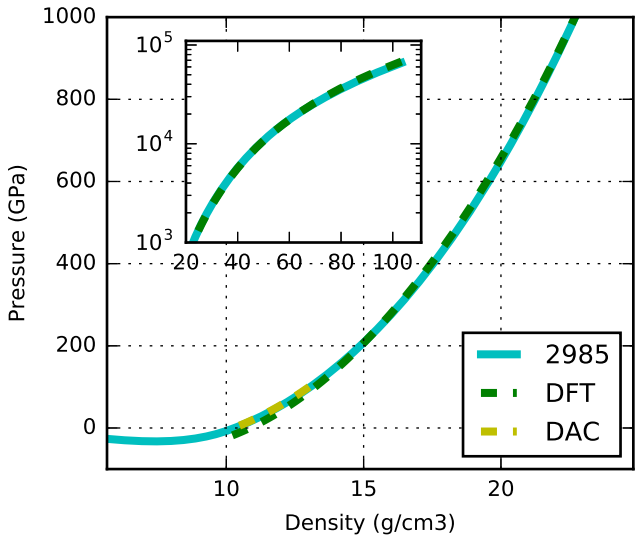

FIG. 1. Cold curve (0K isotherm) for SESAME 2985 derived from full potential DFT simulations of bcc-Mo (AM05 functional, linearized-muffin tin orbital method) and extrapolation of room temperature diamond anvil cell measurements to 0K via Ref. 6.

A Lindemann melt model is used to determine the temperature of transition to liquid EOS. We have taken the assessment of available experimental and theoretical studies given by Wang et al. in Ref. 16 to determine the best estimated range for the Mo melt line. SESAME 2985 gives a better agreement with the available data

[a)] Electronic mail: jbjorgaard@lanl.gov
[b)] Electronic mail: jw@lanl.gov
[c)] Electronic mail: crockett@lanl.gov
[d)] Electronic mail: danielsheppard@lanl.gov

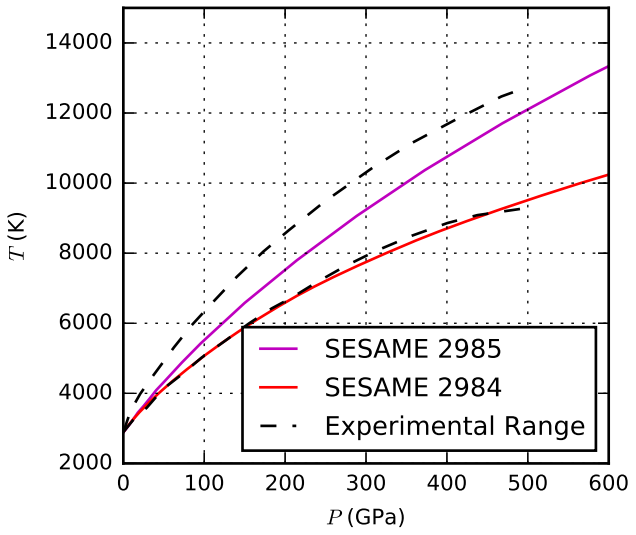

FIG. 2. Melt line interpolated from SESAME 2985 and SESAME 2984 compared with the range of values given in Ref. 16.

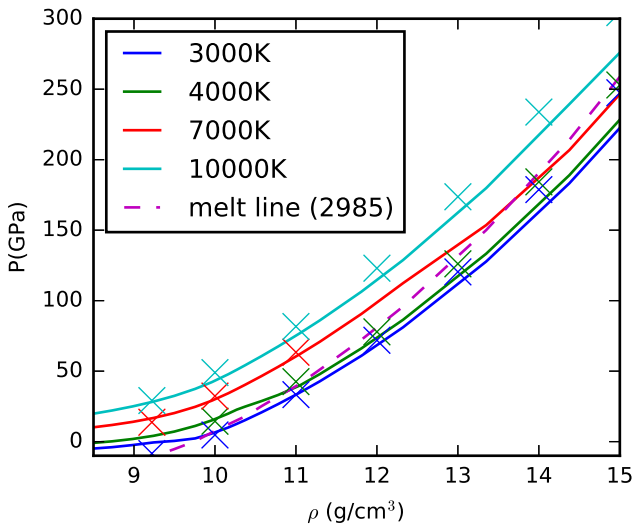

FIG. 3. Liquid isotherms from QMD calculations (x) compared with isotherms from SESAME 2985 (lines) and the melt line from SESAME 2985 (dashed line).

than SESAME 2984, as shown in Fig. 2. The range of melt data at high pressure for Mo is a debated topic and large differences between shock and DAC melting have been observed.[10,11,16–20] Recent experiments have suggested that low temperature melting observed in DAC measurements is due to microstructural transformation.[7] With a wide range of possible melt temperatures at high pressure, we've chosen to match the range near it's mean.

Quantum molecular dynamics (QMD)[21] were performed with the VASP package[22–24] to assess the liquid EOS of SESAME 2985. A cell of 256 randomly distributed Mo atoms was prepared. Molecular dynamics in the isokinetic ensemble were performed to 20 ps with a time step of 1 fs. Equilibration was determined by observing that the moving average of the internal energy became stable. The average pressure after equilibration was shifted down by 15 GPa to account for error in the DFT exchange-correlation functional. The result is plotted in Figure 3 for a range of densities and temperatures. Liquid QMD agrees well with the isotherms from SESAME 2985 in the liquid region of the table. When the melt line crosses the 3000K and 4000K isotherms, the liquid QMD results deviate from the table. The 10000K isotherm also deviates from the table at high pressure, but does not cross the melt line. This may be an effect related to the frozen core approximation used with the pseudopotential in VASP.

The $U_{ion}(\rho, P, T)$ is defined by the 'JDJNuc' model, which smoothly interpolates between gas, solid, and liquid.[8,12] In reference to experimentally determined parameters, we set the Grunweisen parameter to be 1.75 from Ref. 2 and Debye temperature to be 474K.[25] Unlike SESAME 2984, the SESAME 2985 table has been designed to accurately interpolate the low temperature and pressure regime by spacing the temperature grid over 50K increments from 0K to 800K. The comparison to experimental data is shown in Fig. 3. The heat capacity and thermal expansion data match SESAME 2985 well, but begin to diverge near 1500K. The deviation between the EOS and experiments above this temperature could be due to microstructural effects in the Mo samples. At low temperature, SESAME 2985 provides better interpolation than SESAME 2984, which is not able to capture the low temperature isobaric properties.

Our final assessment of SESAME 2985 is of the available Hugoniot data. The Rankine-Hugoniot jump conditions describe the states on either side of a shock wave by

$$U - U_0 = \frac{1}{2}(P + P_0)(\bar{V} - \bar{V}_0) \qquad (2)$$

where U is the internal energy, P is the pressure, and the specific volume is the reciprocal of the density $\bar{V} = 1/\rho$. The given initial conditions combined with the equation of state give the possible final shock states of the material. To interrogate the EOS and determine these states requires solving Eq. 2 by interpolating the EOS table to determine $U(P, \rho)$. This can be done by providing either initial ρ or P points. Many shock wave experiments have been performed on Mo, including measurements of the principle, porous, and heated Hugoniots. We have compared SESAME 2984 and 2985 with all available Hugoniot data in Fig. 5.

The Hugoniot curve is strongly affected by the choice of cold curve. The cold curve of SESAME 2985, generated using full potential DFT calculations at high pressure, produces a Hugoniot which is closer to ultra-high pres-

sure shock data than the cold curve used in SESAME 2984. This is likely due to the cold curve of SESAME 2984 being fit to low pressure Hugoniot data. The uncertainty in the Hugoniot points generated in nuclear tests (all points above 900 GPa) is large, on the order of 1 TPa and 5 g/cm^3. Both SESAME 2984 and SESAME 2985 are within the error bounds of these ultra-high pressure experiments, but it is worth noting that the principle Hugoniot of SESAME 2984 runs below all points above 900 GPa. Heated Hugoniot experiments are available which have an initial temperature of 1673K. As pressure is increased, the experimental data is in better agreement with SESAME 2985 than with SESAME 2984.

Under expansion, the cold curve is matched to a Leonard-Jones type potential where the energy, pressure, and pressure derivative are fit to the Burch-Murnaghan cold curve at a compression of 0.99 and cohesive energy of 176.5 kcal/mol. The accuracy of SESAME 2985 in this regime is determined by comparing it to available porous Hugoniot data as shown in Fig. 6. and to the range of experimental values given in Ref. 26 for the critical temperature and critical pressure. SESAME 2985 has a critical point at 1.1 g/cm^3, 0.23 GPa, and 10600K, which is within the range of experimental values. The critical isotherm has been added to the grid of SESAME 2985 so that interpolation is not necessary at the critical point. The calculated porous Hugoniot poorly matches the experimental data except at low porosity. Due to well known difficulties in the measurement technique and possibility that the EOS model is inaccurate in the low density regime, the discrepancy is acceptable. Further work on adequately representing the low density regime may be carried out in the future.

In summary, SESAME 2985 has several advantages over SESAME 2984. It better matches the ultra-high pressure regime and heated Hugoniot data. It predicts more accurate isobaric properties by better tuning of the model and a finer grid in the low temperature regime. It also provides a better estimate of the high pressure melt line based on up-to-date experimental information. Both SESAME 2984 and SESAME 2985 fail to match measurements of isobaric properties as the melting temperature is approached and both disagree with low density Hugoniot data. Nonetheless, SESAME 2985 is an important update to the SESAME library and significantly improves on SESAME 2984.

[1] G. H. Miller, T. J. Ahrens, and E. M. Stolper, "The equation of state of molybdenum at 1400 C," J. Appl. Phys. **63**, 4469 (1988).

[2] Y. Zhao, A. C. Lawson, J. Zhang, B. I. Bennett, and R. B. Von Dreele, "Thermoelastic squation of state of molybdenum," Phys. Rev. B **62**, 8766 (2000).

[3] T. S. Duffy, G. Shen, J. Shu, H.-K. Mao, R. J. Hemley, and A. K. Singh, "Elasticity, shear strength, and equation of state of molybdenum and gold from x-ray diffraction under nonhydrostatic compression to 24 GPa," J. Appl. Phys. **86**, 6729 (1999).

[4] S. P. Lyon and J. D. Johnson, "SESAME: The Los Alamos National Laboratory equation of state database," Tech. Rep. (LANL, 1992) LA-UR-92-3407.

[5] R. F. Trunin, L. F. Gudarenko, M. V. Zhernokletov, and G. V. Simakov, "Experimental data on shock compression and adiabatic expansion of condensed matter," RFNC-VNIIEF, Sarov **446** (2001).

[6] D. A. Young, H. Cynn, P. Söderlind, and A. Landa, "Zero-kelvin compression isotherms of the elements 1≤Z≥92 to 100 GPa," J. Phys. Chem. Ref. Data **45**, 43101 (2016).

[7] R. Hrubiak, Y. Meng, and G. Shen, "Microstructures define melting of molybdenum at high pressures," Nat. Comm. **8**, 14562 (2017).

[8] T. Sjostrom, S. Crockett, and S. Rudin, "Multiphase aluminum equations of state via density functional theory," Phys. Rev. B **94**, 144101 (2016).

[9] J. C. Boettger, "Relativistic effects on the structural phase stability of molybdenum," J. Phys.: Cond. Matter **11**, 3237 (1999).

[10] A. B. Belonoshko, L. Burakovsky, S. P. Chen, B. Johansson, A. S. Mikhaylushkin, D. L. Preston, S. I. Simak, and D. C. Swift, "Molybdenum at high pressure and temperature: melting from another solid phase," Phys. Rev. Lett. **100**, 135701 (2008).

[11] A. B. Belonoshko, S. I. Simak, A. E. Kochetov, B. Johansson, L. Burakovsky, and D. L. Preston, "High-pressure melting of molybdenum," Phys. Rev. Lett. **92**, 195701 (2004).

[12] D. C. George, "OpenSESAME user manual," Tech. Rep. (LANL, 2004) LA-UR-04-1585.

[13] J. M. Wills, M. Alouani, P. Andersson, A. Delin, O. Eriksson, and O. Grechnyev, *Full–potential electronic structure method: energy and force calculations with density functional and dynamical mean field theory* (Springer Science & Business Media, 2010).

[14] A. E. Mattsson, R. Armiento, J. Paier, G. Kresse, J. M. Wills, and T. R. Mattsson, "The AM05 density functional applied to solids," J. Chem. Phys. **128**, 84714 (2008).

[15] A. Dewaele, M. Torrent, P. Loubeyre, and M. Mezouar, "Compression curves of transition metals in the Mbar range: Experiments and projector augmented-wave calculations," Phys. Rev. B **78**, 104102 (2008).

[16] J. Wang, F. Coppari, R. F. Smith, J. H. Eggert, A. E. Lazicki, D. E. Fratanduono, J. R. Rygg, T. R. Boehly, G. W. Collins, and T. S. Duffy, "X-ray diffraction of molybdenum under shock compression to 450 GPa," Phys. Rev. B **92**, 174114 (2015).

[17] J. H. Nguyen, M. C. Akin, R. Chau, D. E. Fratanduono, W. P. Ambrose, O. V. Fat'yanov, P. D. Asimow, and N. C. Holmes, "Molybdenum sound velocity and shear modulus softening under shock compression," Phys. Rev. B **89**, 174109 (2014).

[18] D. Errandonea, R. Boehler, and M. Ross, "Comment on "Molybdenum sound velocity and shear modulus softening under shock compression"," Phys. Rev. B **92**, 26101 (2015).

[19] J. H. Nguyen, M. C. Akin, R. Chau, D. E. Fratanduono, W. P. Ambrose, O. V. Fat'yanov, P. D. Asimow, and N. C. Holmes, "Reply to "Comment on 'Molybdenum sound velocity and shear modulus softening under shock compression'"," Phys. Rev. B **92**, 26102 (2015).

[20] J. Wang, F. Coppari, R. F. Smith, J. H. Eggert, A. E. Lazicki, D. E. Fratanduono, J. R. Rygg, T. R. Boehly, G. W. Collins, and T. S. Duffy, "X-ray diffraction of molybdenum under ramp compression to 1 TPa," Phys. Rev. B **94**, 104102 (2016).

[21] D. Sheppard, S. Mazevet, F. J. Cherne, R. C. Albers, K. Kadau, T. C. Germann, J. D. Kress, and L. A. Collins, "Dynamical and transport properties of liquid gallium at high pressures," Phys. Rev. E **91**, 63101 (2015).

[22] G. Kresse and J. Furthmüller, "Efficient iterative schemes for ab initio total-energy calculations using a plane-wave basis set," Phys. Rev. B **54**, 11169 (1996).

[23] G. Kresse and J. Furthmüller, "Efficiency of ab-initio total energy calculations for metals and semiconductors using a plane-wave basis set," Comput. Mater. Sci. **6**, 15–50 (1996).

[24] G. Kresse and J. Hafner, "Ab initio molecular-dynamics simulation of the liquid-metal–amorphous-semiconductor transition in germanium," Phys. Rev. B **49**, 14251 (1994).

[25] F. H. Featherston and J. R. Neighbours, "Elastic constants of tantalum, tungsten, and molybdenum," Phys. Rev. **130**, 1324 (1963).

[26]A. N. Emelyanov, A. A. Pyalling, and V. Y. Ternovoi, "Investigation of near–critical states of molybdenum by method of isentropic expansion," International J. Thermophys. **26**, 1985 (2005).
[27]J. M. Dickinson and P. E. Armstrong, "Temperature dependence of the elastic constants of molybdenum," J. Appl. Phys. **38**, 602 (1967).
[28]V. Y. Chekhovskoyi and V. A. Petukhov, "Measurement of thermal expansion of solids at high temperatures," (Inst. for High Temperatures, Moscow, 1970).
[29]W. C. Hubbell and F. R. Brotzen, "Elastic constants of niobium-molybdenum alloys in the temperature range -190 to +100 C," J. Appl. Phy. **43**, 3306 (1972).
[30]F. I. Dolinin, E. Z. Kuchinskij, and E. A. Pamyatnykh, "Thermal expansion of metals at low temperatures," Fizika Metallov i Metallovedeniya , 5 (1990).
[31]G. A. Mochalov and O. S. Ivanov, "High-temperature vacuum dilatometer with optical measurement of specimen length," Indust. Lab. **35**, 139 (1969).
[32]M. P. Arbuzov and I. A. Zelenkov, "Thermal expansion of certain transition metals and alloys on their base," Fiz Met Metalloved **18**, 311 (1964).
[33]D. L. Davidson, *The properties of solid solution, molybdenum-rich Mo-Rh alloys from -190 to +100 C*, PhD Thesis, Rice University (1968).
[34]F. C. Nix and D. MacNair, "The thermal expansion of pure metals. II: molybdenum, palladium, silver, tantalum, tungsten, platinum, and lead," Phys. Rev. **61**, 74 (1942).
[35]P. Hidnert and W. B. Gero, "Thermal expansion of molybdenum," Tech. Rep. (1924).
[36]D. Clark and D. Knight, "The thermal expansion of beta–silicon carbide and some tungstem–molybdenum alloys," Tech. Rep. (Royal Aircraft Establishment, Farnborough UK, 1965).
[37]J. Valentich, "Thermal expansion measurement," Instrument Control Systems **42**, 91 (1969).
[38]L. W. Schad and P. Hidnert, *Preliminary determination of the thermal expansion of molybdenum*, 332 (Govt. Print. Off., 1919).
[39]C. Lucks and H. Deem, "Thermal properties of thirteen metals," (ASTM International, 1958).
[40]N. S. Rasor and J. D. McClelland, "Thermal properties of materials. part I. properties of graphite, molybdenum, and tantalum to their destruction temperatures," US Air Force Rept. WADC-TR-56-400, Pt. I (1957).
[41]A. G. Worthing, "Physical properties of well seasoned molybdenum and tantalum as a function of temperature," Phys. Rev. **28**, 190 (1926).
[42]C. F. Lucks and H. W. Deem, "Thermal conductivities, heat capacities, and linear thermal expansion of five materials," Tech. Rep. (Battelle Memorial Inst., Columbus, Ohio, 1956).
[43]I. B. Fieldhouse and J. I. Lang, "Measurement of thermal properties," Tech. Rep. (Armour Research Foundation Chicago IL, 1961).
[44]G. L. Denman, "An automatic recording dilatometer for thermal expansion measurements to 2000 F," Tech. Rep. (Aeronautical Systems Div. Wright-Patterson AFB, OH, 1962).
[45]M. A. Levinstein, A. Eisenlohr, and B. E. Kramer, "Properties of plasma-sprayed materials," Welding J. (NY) **40** (1961).
[46]E. E. Totskii, "Experimental determination of the coefficient of linear expansion of metals and alloys," High Temp. **2**, 181 (1964).
[47]J. W. Edwards, R. Speiser, and H. L. Johnston, "High temperature structure and thermal expansion of some metals as determined by X-ray diffraction data. I. Platinum, tantalum, niobium, and molybdenum," J. Appl. Phys. **22**, 424 (1951).
[48]V. M. Amonenko, P. N. V'yugov, and V. S. Gumenyuk, "Thermal expansion of tungsten, molybdenum, tantalum, niobium, and zirconium at high temperatures," High Temp. **2** (1964).
[49]R. G. Ross and W. Hume-Rothery, "High temperature X-ray metallography: I. A new debye-scherrer camera for use at very high temperatures II. A new parafocusing camera III. Applications to the study of chromium, hafnium, molybdenum, rhodium, ruthenium and tungsten," J. Less Common Metals **5**, 258 (1963).
[50]R. R. Pawar, "Lattice expansion of molybdenum," Curr. Sci. **36**, 428 (1967).
[51]J. B. Conway and A. C. Losekamp, "Thermal–expansion characteristics of several refractory metals to 2500 c," Trans. Met. Soc. AIME **236** (1966).
[52]I. N. Frantsvich, E. A. Zhurakovskii, and A. B. Lyashchenko, "Elastic constants and characteristics of the electron structure of certain classes of refractory compounds obtained by the metal-powder method," Inorg. Mater. **3**, 6 (1967).
[53]M. E. Straumanis and C. L. Woodward, "Lattice parameters and thermal expansion coefficients of Al, Ag and Mo at low temperatures. Comparison with dilatometric data," Acta Cryst. Sec. A **27**, 549 (1971).
[54]C. P. Butler and E. C. Y. Inn, "A radiometric method for determining specific heat at elevated temperatures," Tech. Rep. (Naval Radiological Defense Lab., San Francisco, 1958).
[55]J. H. Boggs and J. A. Wiebelt, "An investigation of a particular comparative method of specific heat determination in the temperature range of 1500 F to 2600 F," Tech. Rep. (Oklahoma State Univ., Stillwater. School of Mechanical Engineering, 1960).
[56]F. M. Jaeger and W. A. Veenstra, "The exact measurement of the specific heats of solid substances at high temperatures. VI. The specific heats of vanadium, niobium, tantalum and molybdenum," Recueil des Travaux Chimiques des Pays-Bas **53**, 677 (1934).
[57]R. L. Rudkin, W. J. Parker, and R. J. Jenkins, "Measurements of the thermal properties of metals at elevated temperatures," Temp. Meas. Control Sci. Ind. **3** (1962).
[58]T. A. Redfield and J. H. Hill, "Heat capacity of molybdenum," Tech. Rep. (Oak Ridge National Lab., 1951).
[59]R. E. Taylor and R. A. Finch, "The specific heats and resistivities of molybdenum, tantalum and rhenium from low to very high temperatures," Tech. Rep. (Atomics International. Div. of North American Aviation, Inc., Canoga Park, Calif., 1961).
[60]G. C. Lowentha, "The specific heat of metals between 1200 K and 2400 K," Australian J. Phys. **16**, 47 (1963).
[61]J. A. Cape and R. E. Taylor, "Thermal properties of refractory materials," Tech. Rep. (Atomics International. Div. of North American Aviation, Inc., Canoga Park, Calif., 1961).
[62]V. A. Kirillin, A. E. Sheindlin, and V. Y. Chekhovskoi, "Experimental determinaton of the enthalpy and heat capacity of molybdenum up to 2337 C," Int. J. Heat and Mass Trans. **5**, 1 (1962).
[63]L. S. Lazareva, P. B. Kantor, and V. V. Kandyba, "Enthalpy and heat capacity of molbydenum in the 1200-2500 K temperature range," Tech. Rep. (Air Force Systems Command Wright-Patterson AFB, OH Foreign Technology Division, 1961).
[64]G. W. Lehman, "Thermal properties of refractory materials," Tech. Rep. (Atomics International. Div. of North American Aviation, Inc., Canoga Park, Calif., 1960).
[65]D. C. Rorer, *Thermodynamic properties of superconducting and normal molybdenum*, PhD Thesis, Duke University (1964).
[66]H. Ralph, *Selected values of thermodynamic properties of metals and alloys* (Wiley New York, 1963).
[67]M. P. Arbuzov and I. A. Zelenkov, "Thermal expansion of certain transition metals and alloys on their base," Fiz Met Metalloved **18**, 311 (1964).
[68]Retrieved from CINDAS LLC Thermophysical Properties of Matter Database (TPMD). Version 10.0 at http://cindasdata.com/.
[69]S. P. Marsh, *LASL shock Hugoniot data*, Vol. 5 (Univ. of California Press, 1980).
[70]M. Van Thiel, J. Shaner, and E. Salinas, "Compendium of shock wave data. compendium index," Tech. Rep. (Lawrence Livermore National Lab, 1977).

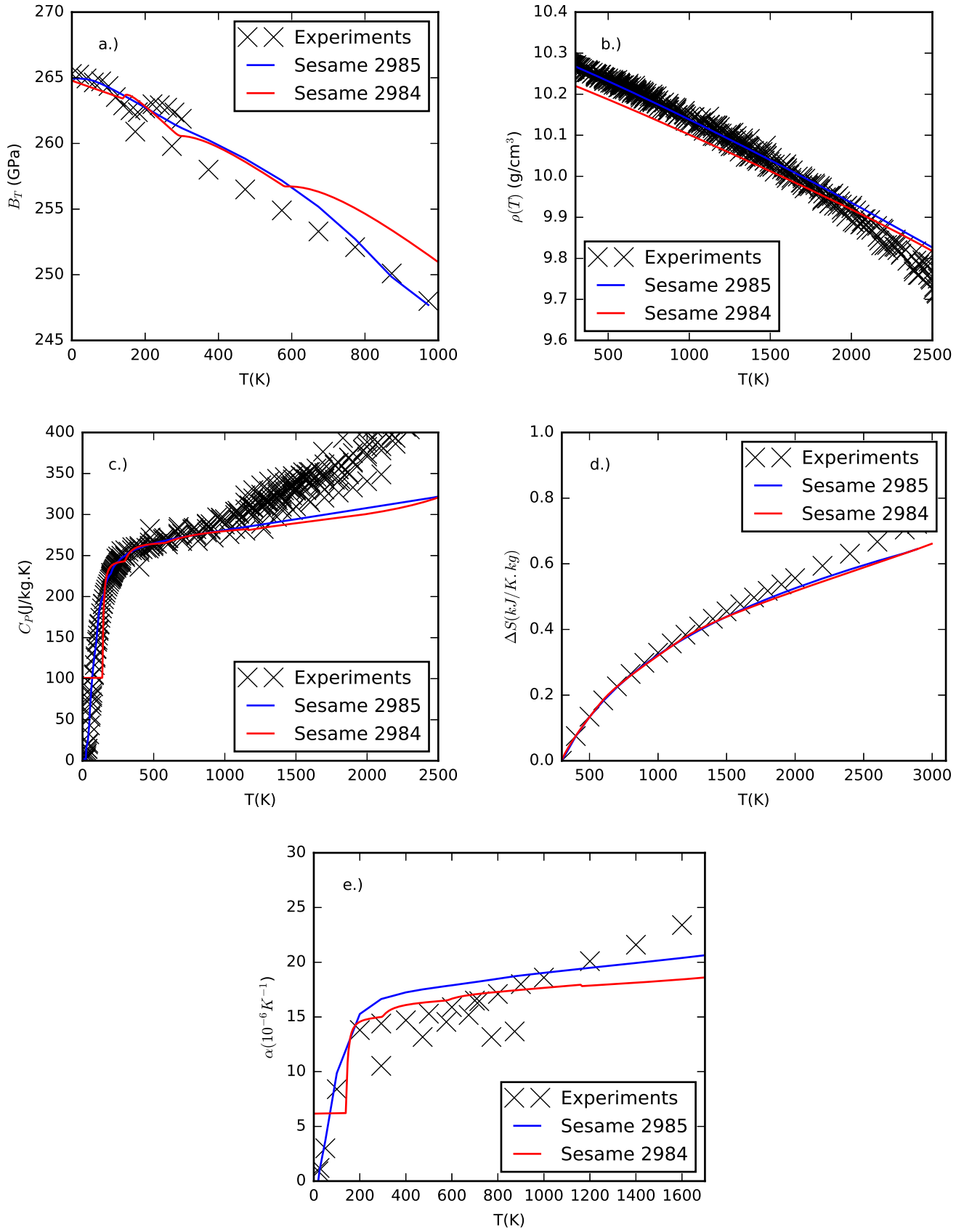

FIG. 4. Isobaric data for SESAME tables 2984 and 2985 matched with available experiments. a.) Bulk modulus from experiments[25,27] compared with SESAME tables. b.) Experimental density is determined from linear expansion data[28–53] and a reference (RT) density of 10.2686. c.) Heat capacity data[39,54–65] d.) Entropy as a function of temperature from Ref. 66 e.)Thermal expansion coefficient from experiment[67] and CINDAS database recommended values.[68]

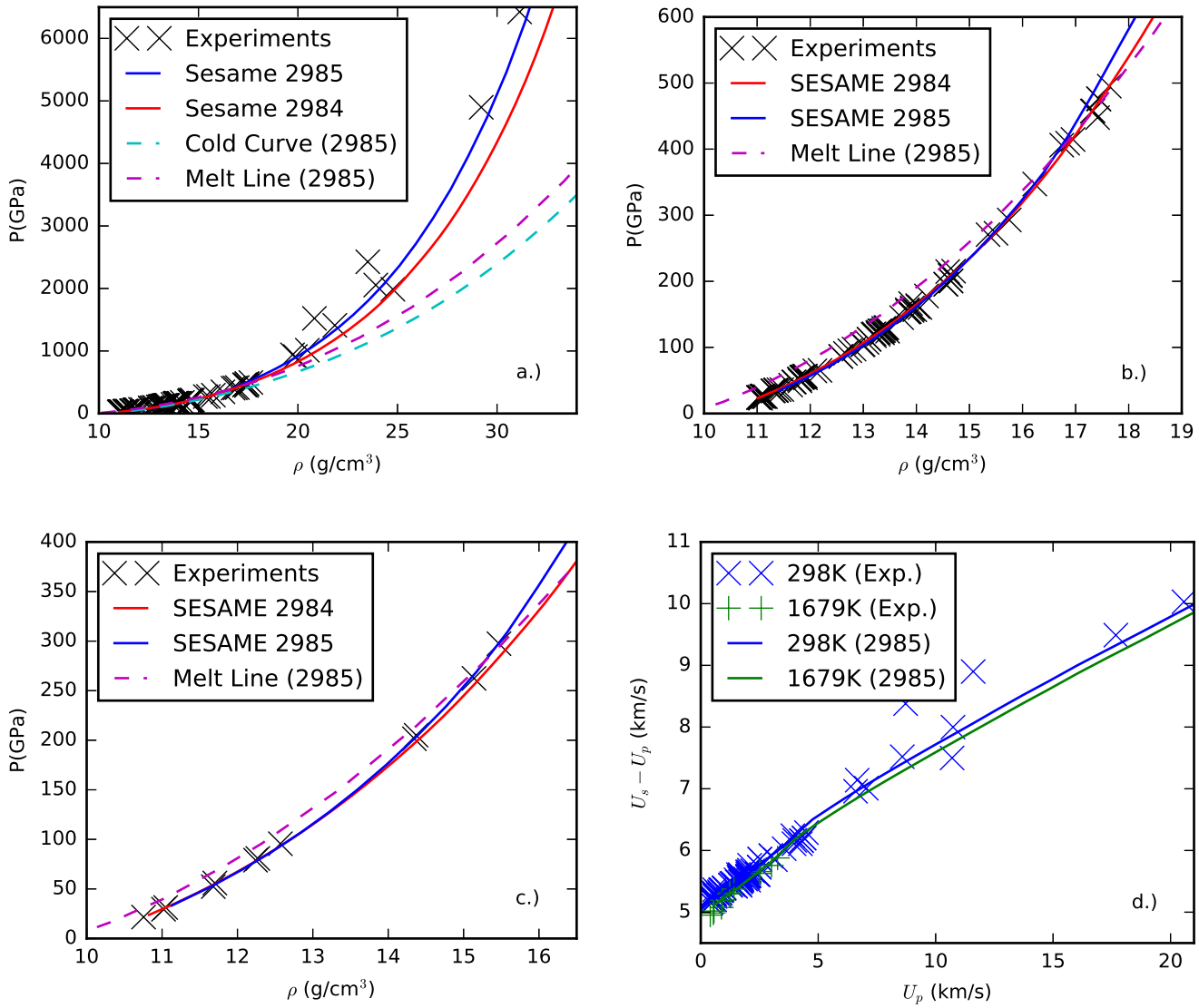

FIG. 5. a.) Principle Hugoniot in the ultra-high pressure regime plotted with cold curve and melt line from SESAME 2985. b.) Principle Hugoniot up to 600 GPa plotted with the melt line from SESAME 2985. c.) Heated Hugoniot with initial temperature of 1673K plotted with the melt line from SESAME 2985. d.) Shock and particle velocities for principle and heated Hugoniot. Experimental data is from Refs. 5, 69, and 70

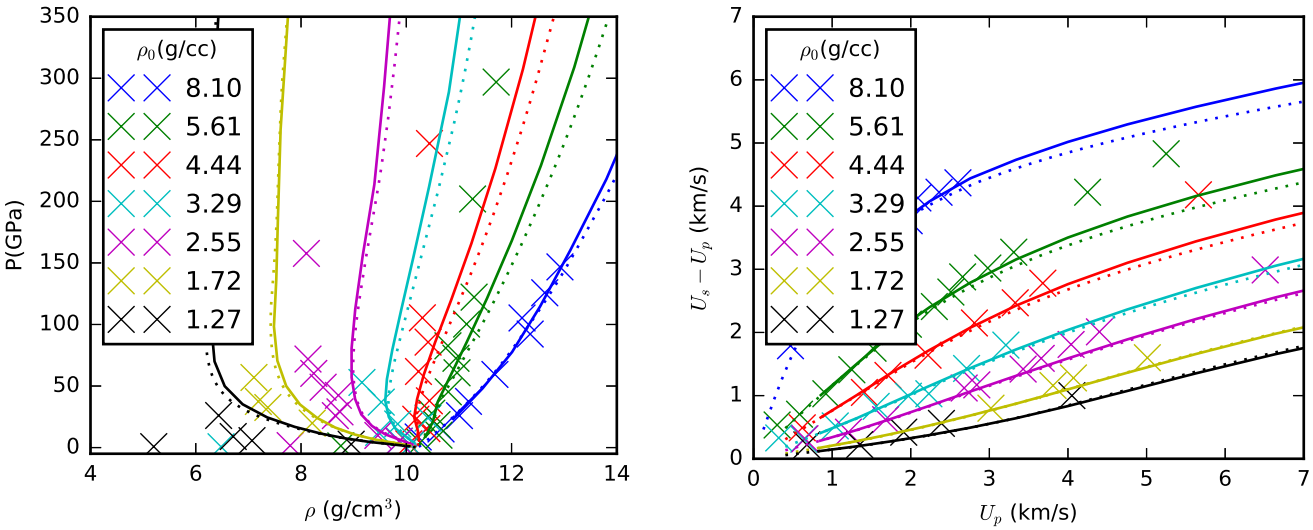

FIG. 6. Porous hugoniot data[5] compared with SESAME 2984 (dotted lines) and 2985 (solid lines).